

Electronic Supplementary Information (ESI):

**Nanoporous Sr-rich strontium titanate: a stable and superior
photocatalyst for H₂ evolution**

Liang-Liang Feng,^a Xiaoxin Zou,^{a,b,*} Jun Zhao,^a Li-Jing Zhou,^a De-Jun Wang,^{a,c} and Guo-Dong Li^{a,*}

^a State Key Laboratory of Inorganic Synthesis and Preparative Chemistry, Jilin University, Changchun 130012, P.R. China

^b Department of Chemistry and Chemical Biology, Rutgers, The State University of New Jersey, NJ 08854, USA.

^c Department of Chemistry, Tsinghua University, Beijing 100084, P. R. China

* E-mail: G. D. Li, lgd@jlu.edu.cn;

X. X. Zou, chemistryzoux@ gmail.com

Experimental section

Synthesis of SrTiO₃-1: For the synthesis of SrTiO₃-1, 0.01 mol Sr(NO₃)₂ and 0.04 mol citric acid were added into 10 mL H₂O to form solution **1**; and 0.005-0.0067 mol titanium tetrabutoxide was added into 4 mL ethylene glycol to form solution **2**. Solutions **1** and **2** were mixed and heated at 70 °C for 3 h, and the resulting solution was transferred and kept in an oven at 120 °C for 24 h, finally leading to the formation of a spongy solid product. This solid product was thermally treated in air at 200 °C (6 h), 300 °C (6h), 500 °C (3 h) and 600 °C (6 h) in succession with a heating rate of 1.7 °C/min. After cooling to room temperature, the obtained product was treated with 1 M HCl for 6 h, and then the solution was centrifuged to recover a white precipitate, which was washed several times with water and dried in an oven at 60 °C, resulting in SrTiO₃-1.

Synthesis of SrTiO₃-2: For the synthesis of SrTiO₃-2, 0.01 mol Sr(NO₃)₂ and 0.04 mol citric acid were added into 10 mL H₂O to form solution **1**; and 0.01 mol titanium tetrabutoxide was added in 4 mL ethylene glycol to form solution **2**. Solutions **1** and **2** were mixed and heated at 70 °C for 3 h, and the resulting solution was transferred and kept in an oven at 120 °C for 24 h, finally leading to the formation of a spongy solid product. This solid product was thermally treated in air at 200 °C (6 h), 300 °C (6h), 500 °C (3 h) and 600 °C (6 h) in succession with a heating rate of 1.7 °C/min. The finally obtained solid product is the SrTiO₃-2 sample.

Synthesis of porous SrZrO₃: For the synthesis of porous SrZrO₃, 0.01 mol Sr(NO₃)₂, 0.0067 mol ZrOCl₂·8H₂O and 0.04 mol citric acid were first added into 10 mL H₂O at 50 °C to form transparent solution **1**. Then, 4 mL ethylene glycol was added into the solution **1** to form a new solution **2**. Solution **2** was heated at 70 °C for 3 h, and the resulting solution was transferred and kept in an oven at 120 °C for 12 h, finally leading to the formation of a spongy solid product. This solid product was thermally treated in air at 200 °C (6 h), 300 °C (6h), 500 °C (3 h) and 600 °C (6 h) in succession with a heating rate of 1.7 °C/min. After cooling to room temperature, the obtained product was treated with 1 M HCl for 6 h, and then the solution was centrifuged to recover a white precipitate, which was washed several times with water and dried in an oven at 60 °C, resulting in the formation of porous SrZrO₃ (see detailed characterizations in Fig. S8).

General Characterization: The powder X-ray diffraction (XRD) patterns were recorded on a Rigaku D/Max 2550 X-ray diffractometer using CuKa radiation ($\lambda = 1.5418 \text{ \AA}$) operated at 200 mA and 50 kV. The transmission electron microscopy (TEM) and high-resolution TEM (HRTEM) images were obtained on a Philips-FEI Tecnai G2S-Twin with a field emission gun operating at 200 kv. The Brunauer-Emmett-Teller surface areas and Nitrogen adsorption- desorption isotherms of the samples were measured by using a Micromeritics ASAP 2020M system. The X-ray photoelectron spectroscopy (XPS) was performed on an ESCALAB 250 X-ray photoelectron spectrometer with a monochromated X-ray source (Al KR $h\nu = 1486.6 \text{ eV}$). The UV/Vis diffuse reflectance spectra were recorded on a Perkin-Elmer Lambda 20 UV/Vis spectrometer. The surface photovoltaic spectroscopy (SPS) measurement was performed on home-made surface photovoltaic equipment. The SPS measurement system consisted of a source of monochromatic light, a lock-in amplifier with a light chopper, a photovoltaic cell, and a computer. A 500 W xenon lamp and a grating monochromator were combined to provide the monochromatic light. A low chopping frequency of ~23 Hz was used. The photovoltaic cell was a sandwich-like structure consisting of ITO-sample-ITO.

Evaluation of photocatalytic activity: The photocatalytic activities of these samples were evaluated by photocatalytic H₂ evolution. The photocatalytic reaction was performed in a quartz cell, which was connected with a closed gas circulation system and irradiated from an external light source. The light source was a 500 W Xe lamp.

A photocatalyst (30 mg) was added into aqueous methanol solution (50 vol %, 50 mL) in the cell and the aqueous system was magnetically stirred during the whole photocatalytic testing. 1 wt.% Pt co-catalyst was loaded onto the surface of the photocatalyst by an *in situ* photo-deposition method using an appropriate amount of H₂PtCl₆·6H₂O as precursor. Before light irradiation, the system was evacuated to eliminate air and the temperature of the system during photocatalytic reaction was kept around 23 °C by a continuous flow of water. The evolved gases were detected *in situ* using an online gas chromatograph (Shimadzu, GC-2014C, TCD, Molecular sieve 5 Å, Argon gas), which was connected to the system and was equipped with a thermal conductivity detector.

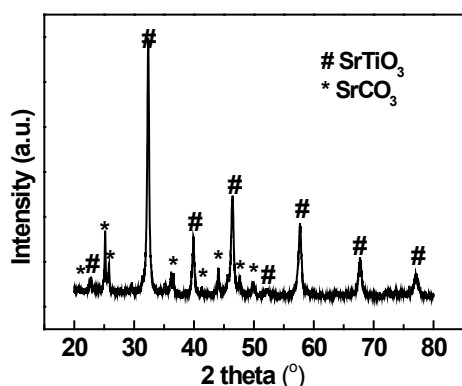


Fig. S1 XRD pattern of the composite of SrTiO₃ and SrCO₃, which was synthesized by a polymerized complex method.

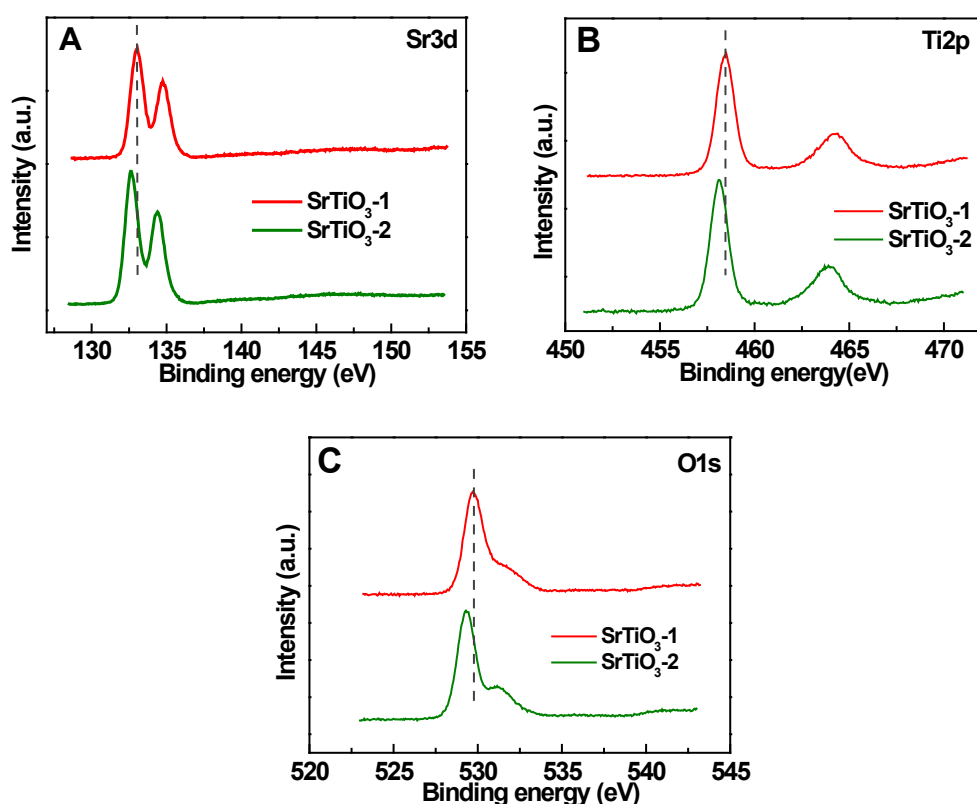


Fig. S2 High-resolution XPS spectra of (A) Sr3d, (B) Ti2p and (C) O1s for SrTiO₃-1 and SrTiO₃-2.

Comparison of the XPS spectra (Fig. S2A-C) revealed that slight shifts of the Sr3d, Ti2p and O1s XPS signals to higher binding energies were observed for SrTiO₃-1 with respect to SrTiO₃-2. This phenomenon is probably because SrTiO₃-1 is a Sr-rich material with a Sr:Ti atomic ratio of ~1.03:1 (1:1 for SrTiO₃-2), and the excess Sr²⁺ ions (with a larger ionic radius than Ti⁴⁺) could be substituted for Ti⁴⁺ ions in SrTiO₃-1.

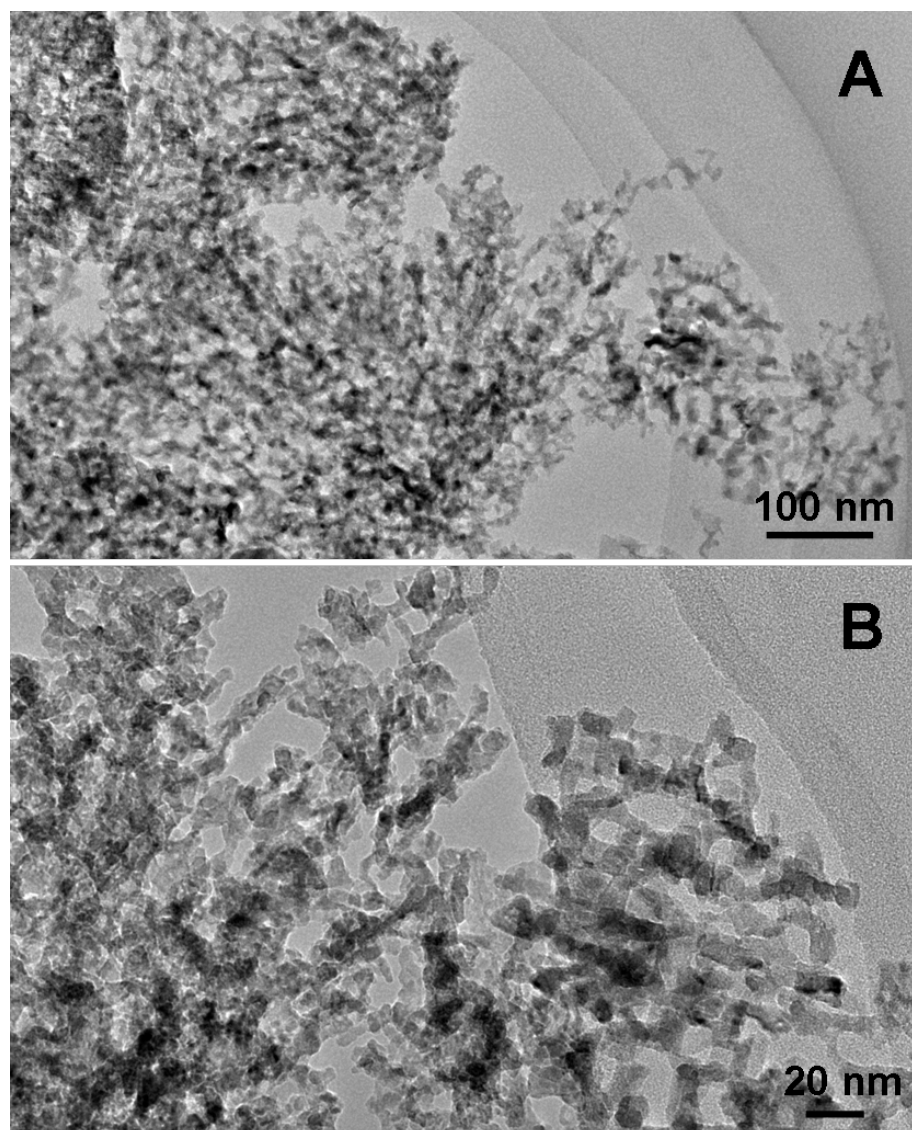


Fig. S3 TEM images of $\text{SrTiO}_3\text{-}1$.

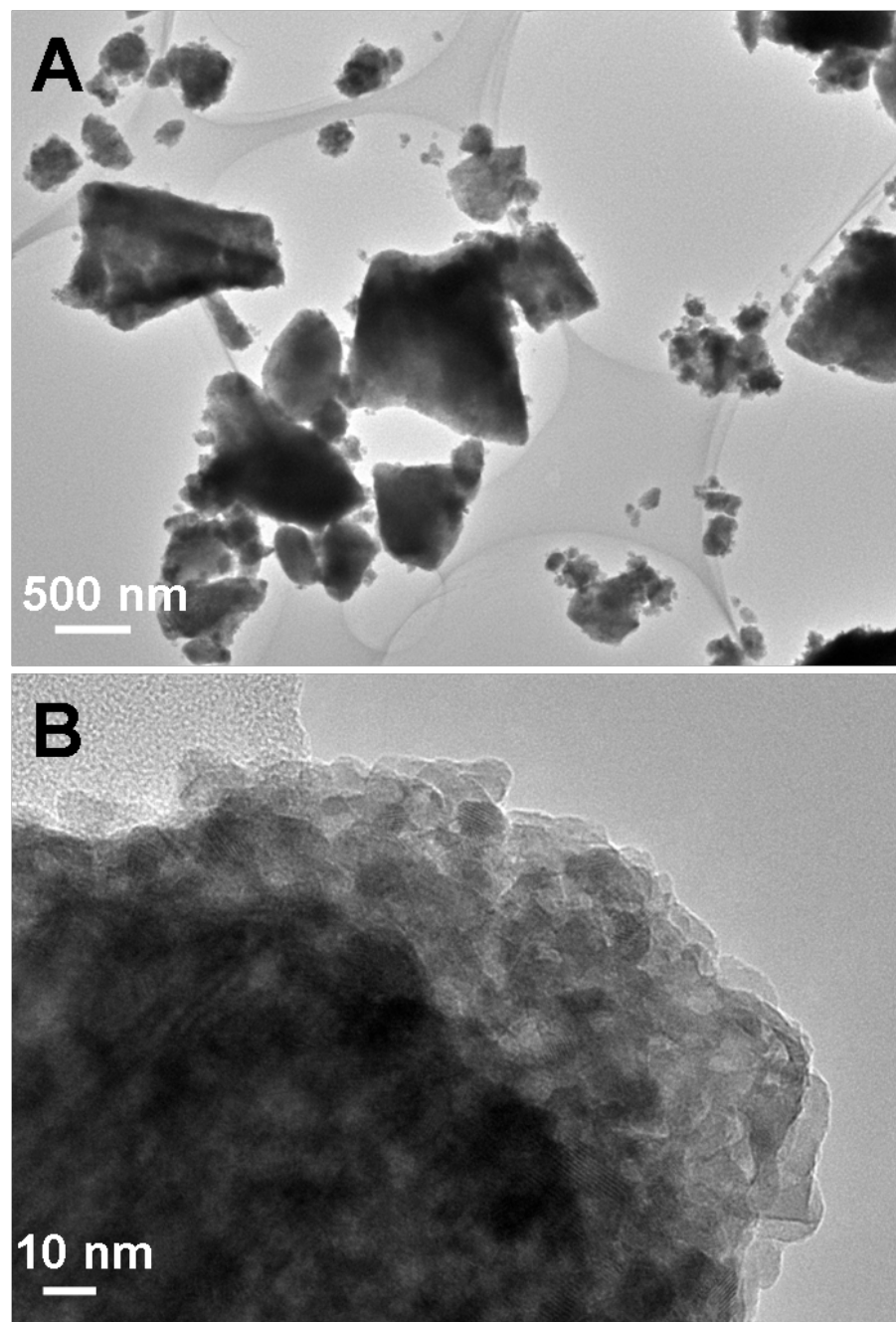


Fig. S4 TEM images of the composite of SrTiO_3 and SrCO_3 .

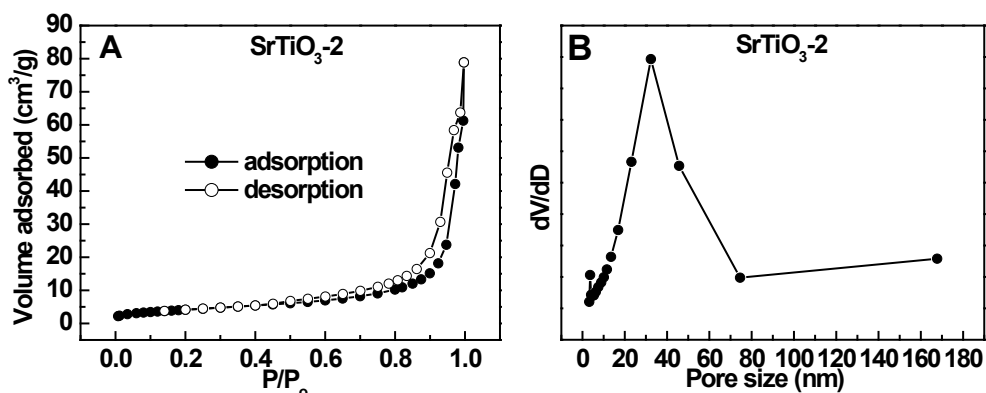


Fig. S5 (A) N₂ adsorption-desorption isotherms of SrTiO₃-2 and (B) the corresponding pore size distribution derived from desorption isotherm.

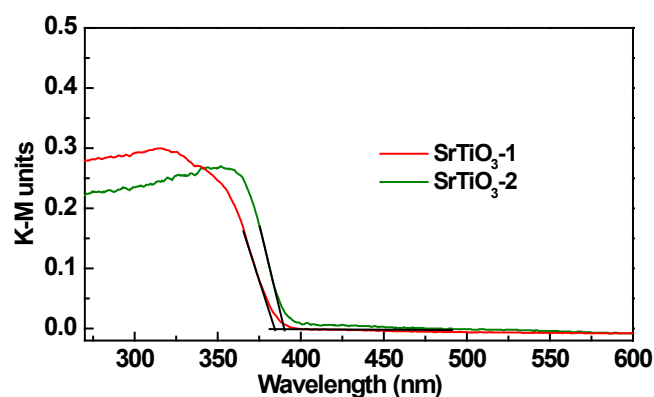


Fig. S6 UV/Vis absorption spectra of SrTiO₃-1 and SrTiO₃-2.

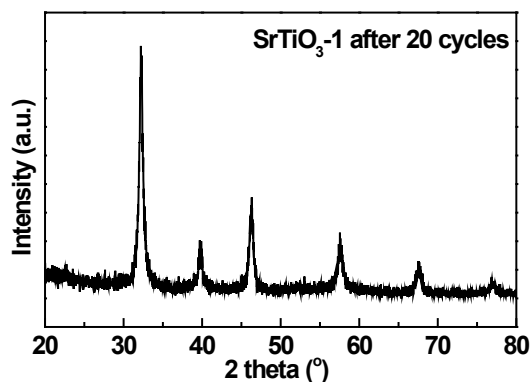


Fig. S7 XRD pattern of SrTiO₃-1 after 20 cycles of the catalytic H₂ evolution.

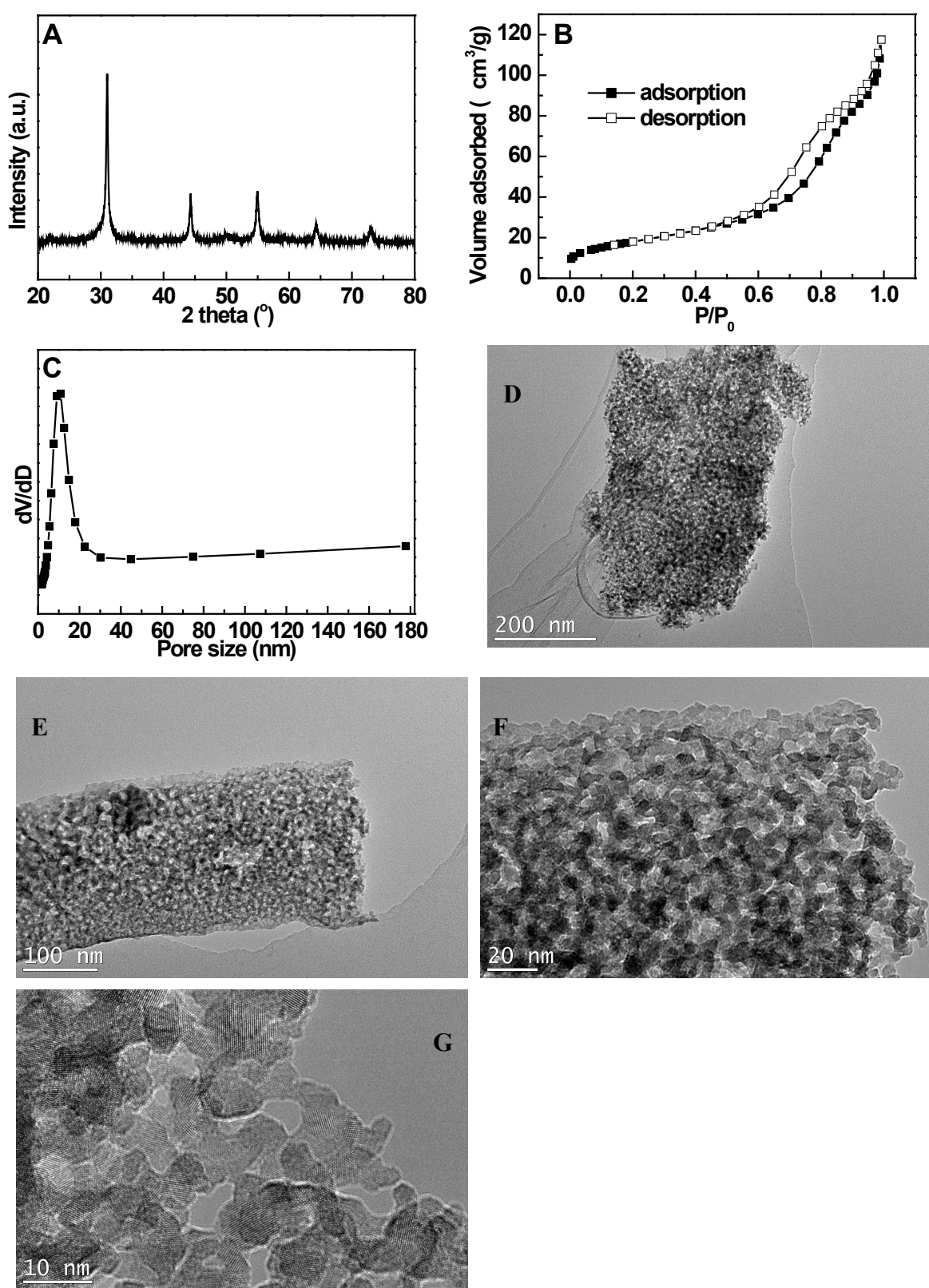


Fig. S8 (A) XRD pattern, (B) N₂ adsorption-desorption isotherms of porous SrZrO₃ and (C) the corresponding pore size distribution derived from the desorption isotherm. (D-G) TEM images of porous SrZrO₃.

Fig. S8A shows that all the XRD peaks of the sample match well with those of perovskite-type SrZrO_3 .^[S1] The N_2 adsorption-desorption isotherms (Fig. S8B) of $\text{SrTiO}_3\text{-}1$ are characteristic of type-IV with H1-type hysteresis loops, demonstrating the presence of mesopores in the material. The corresponding BJH pore-size distribution (Fig. S8C) derived from the desorption isotherm shows a narrow pore-size distribution centered at 9.5 nm. This porous SrZrO_3 possesses a BET surface area of $\sim 70 \text{ m}^2/\text{g}$. The TEM images (Fig. S8D-G) further confirm the existence of porous structure in this SrZrO_3 sample.

ESI references:

- [S1] T. Ye, Z. Dong, Y. Zhao, J. Yu, F. Wang, S. Guo and Y. Zou, *CrystEngComm*, 2011, **13**, 3842.